Interactions of Human Replication Protein A with Oligonucleotides†

Changsoo Kim,‡ Brian F. Paulus,§ and Marc S. Wold*

Department of Biochemistry, University of Iowa College of Medicine, 51 Newton Road, Iowa City, Iowa 52242

Received March 23, 1994; Revised Manuscript Received September 22, 1994®

ABSTRACT: Replication protein A (RPA) is a heterotrimeric, single-stranded DNA binding protein that is essential for eukaryotic DNA replication. In order to gain a better understanding of the interactions between RPA and DNA, we have examined the interactions of human RPA with single-stranded oligonucleotides. Our analysis of RPA·DNA complexes demonstrated that RPA binds as a heterotrimer. Stoichiometric binding reactions monitored by fluorescence quenching indicated that the binding site size of human RPA is 30 nucleotides and that between 20−30 nucleotides of DNA directly interact with RPA. The binding of RPA to DNA of different lengths was systematically examined using deoxythymidine-containing oligonucleotides. We found that the binding affinity of RPA for short oligonucleotides was length dependent. The apparent association constant of RPA varied over 200-fold from $\sim 7 \times 10^7$ M^{-1} for oligo(dT)10 to $\sim 1.5 \times 10^{10}$ M^{-1} for oligo(dT)50. Human RPA binds to oligonucleotides with low cooperativity; the cooperativity parameter (ω) for RPA binding was estimated to be approximately 15.

Proteins that bind to single-stranded DNA exist in all cell types. These proteins are essential for DNA replication and other processes of DNA metabolism (Kornberg & Baker, 1992; Revzin, 1990). Extensive studies of prokaryotic single-stranded DNA-binding proteins have shown that their interactions with DNA are complex (Karpel, 1990; Lohman & Bujalowski, 1990). In addition, several prokaryotic single-stranded DNA-binding proteins participate in specific protein−protein interactions that are important for their function (Karpel, 1990; Lohman & Bujalowski, 1990). Understanding these interactions is essential for understanding the molecular mechanisms of DNA replication, repair and recombination.

In eukaryotes, single-stranded DNA-binding proteins are less well characterized (Williams & Chase, 1990). Initially, the lack of physiological assays hampered the identification of cellular single-stranded DNA-binding proteins (Williams & Chase, 1990). Development of cell-free systems for examining eukaryotic DNA replication and recombination led to the identification of a family of multisubunit, eukaryotic single-stranded DNA-binding proteins (Stillman, 1989; Challberg & Kelly, 1989; Hurwitz *et al.*, 1990). This family was first identified in extracts from human cells (Wobbe *et al.*, 1987; Wold & Kelly, 1988; Fairman & Stillman, 1988) when replication protein A (RPA[1] also known as human SSB and replication factor A) was purified as being essential for SV40 DNA replication *in vitro* (Wobbe *et al.*, 1987; Wold & Kelly, 1988; Fairman & Stillman, 1988). Human RPA is composed of subunits of 70, 32, and 14 kDa (Wold & Kelly, 1988; Fairman & Stillman, 1988) and binds very tightly to single-stranded DNA (ssDNA) (Wobbe *et al.*, 1987; Wold & Kelly, 1988; Fairman & Stillman, 1988). RPA is the major single-stranded DNA-binding protein in mammalian cells (Seroussi & Lavi, 1993). RPA is highly conserved throughout evolution; homologous three-subunit, single-stranded DNA-binding proteins have been found in all eukaryotic cells examined (Heyer *et al.*, 1990; Brill & Stillman, 1991; Erdile *et al.*, 1990, Erdile *et al.*, 1991; Umbricht *et al.*, 1993; Nakagawa *et al.*, 1991; Atrazhev *et al.*, 1992; Adachi & Laemmli, 1992; Georgaki *et al.*, 1992; Mitsis *et al.*, 1993; Fang & Newport, 1993; Brown *et al.*, 1994).

Human RPA is a heterotrimer in solution (Fairman & Stillman, 1988; Kenny *et al.*, 1990). The hRPA complex is very stable, and all three subunits appear to be necessary for RPA function (Wold & Kelly, 1988; Fairman & Stillman, 1988; Erdile *et al.*, 1991; Kenny *et al.*, 1990; Henricksen *et al.*, 1994). The 70-kDa subunit has been shown to have intrinsic ssDNA binding activity (Wold *et al.*, 1989; Kenny *et al.*, 1990; Erdile *et al.*, 1991). The 32- and 14-kDa subunits form a stable subcomplex (Henricksen *et al.*, 1994; Stigger *et al.*, 1994) and are probably important for normal RPA complex formation (Henricksen *et al.*, 1994). The 32-kDa subunit of RPA is a site of cell cycle dependent phosphorylation becoming phosphorylated at the beginning of S-phase (Din *et al.*, 1990). Thus, it is possible that the smaller two subunits of RPA may also be involved in the regulation of RPA function.

In addition to being absolutely required for DNA replication, RPA participates in the processes of DNA repair (Coverley *et al.*, 1991, 1992) and recombination (Heyer *et al.*, 1990; Moore *et al.*, 1991). RPA increases the fidelity of DNA synthesis (Carty *et al.*, 1992, 1993; Roberts *et al.*, 1993) and stimulates the activities of several DNA helicases and DNA polymerases α, δ, and ε (Seo *et al.*, 1991; Thömmes *et al.*, 1992; Tsurimoto & Stillman, 1989; Kenny *et al.*, 1990; Lee *et al.*, 1991; Erdile *et al.*, 1991). RPA specifically interacts with both SV40 large T antigen and

† This work was supported by Public Health Service Grant GM44721 from the National Institute of Health General Medicine Institute.

* To whom correspondence should be sent. Phone: (319) 335-6784. Fax: (319) 335-9570. E-mail: marc-wold@uiowa.edu.

‡ Current address: Department of Biology, California Institute of Technology, Pasadena, CA 91125.

§ Current address: Department of Biochemistry, The Johns Hopkins University, 615 N. Wolfe Street, Baltimore, MD 21205-1109.

® Abstract published in *Advance ACS Abstracts,* November 1, 1994.

[1] Abbreviations RPA, replication protein A; dRPA, *Drosophila melanogaster* replication protein A; scRPA, *Saccharomyces cerevisiae* replication protein A; ssDNA, single-stranded DNA; nt, nucleotides.

0006-2960/94/0433-14197$04.50/0

with DNA polymerase α (Dornreiter *et al.*, 1992). These interactions seem to be important for initiation of DNA replication and primer synthesis (Collins & Kelly, 1991; Murakami *et al.*, 1992; Melendy & Stillman, 1993). Recently, RPA has been shown to also interact with the tumor suppressor p53 and with transcriptional activators such as gal4 and VP16 (Li & Botchan, 1993; He *et al.*, 1993; Dutta *et al.*, 1993). The physiological relevance of these interactions is not yet clear.

In order to further understand the molecular basis of the interaction between RPA and DNA and how these interactions contribute to RPA function in DNA metabolism, more rigorous information about the thermodynamic binding parameters of RPA is required. The binding properties of the RPA homologues from *Saccaromyces cerevisiae* (scRPA) and *Drosophila melanogaster* (dRPA) have been described previously (Alani *et al.*, 1992; Mitsis *et al.*, 1993); however, in those initial studies the binding characteristics of these two homologues were found to be quite different. Both homologues have a high affinity for ssDNA, but dRPA bound with a binding site of 22 nucleotides and low cooperativity, while scRPA had a binding site of ~90 nucleotides and bound with very high cooperativity. In this report, we present our characterization of the interactions of human RPA with oligonucleotides. We demonstrate that the binding site size is 30 nucleotides per RPA heterotrimer and that the interaction site size of RPA is between 20 and 30 nucleotides. We show that RPA binding to ssDNA is length dependent; the binding affinity for oligo(dT)50 is 200-fold higher than for oligo(dT)10, and RPA binds to oligonucleotides with low cooperativity.

EXPERIMENTAL PROCEDURES

Materials. Bovine serum albumin (BSA) was obtained from Boehringer Mannheim Biochemicals. ProtoGel from National Diagnostics (30%/0.8% acrylamide/bisacrylamide, w/v) was used to make polyacrylamide gels. [α-^{32}P]dATP (3000 Ci/mmol), [α-^{32}P]dCTP (3000 Ci/mmol), and [γ-^{32}P]-ATP (4500 Ci/mmol) were obtained from ICN. Restriction enzymes, calf intestinal phosphatase, and DNA polymerase I Klenow fragment were purchased from New England BioLabs and Life Technologies, Inc. T4 polynucleotide kinase and ssDNA cellulose (18 mg of DNA/g of cellulose) were from USB. Affi-Gel blue was from Bio-Rad, and hydroxylapatite was from Calbiochem. Protein standards for hydrodynamic studies were obtained from Pharmacia/LKB.

Oligonucleotides. (dT)10 and (dT)12 were obtained from Pharmacia. (dT)15, (dT)20, (dT)30, (dT)50, (dT)60, and (dT)70 were synthesized by the University of Iowa DNA Core Facility using an Applied Biosystems DNA synthesizer model 380B. Poly(dT) (2000−4000 nucleotides) was from Midland Co. (Midland, TX). Oligonucleotides were 99% pure as judged by autoradiography after separation by electrophoresis of ^{32}P-end-labeled DNA through a 10% sequencing gel. The concentrations of the deoxythymidine oligo- and polynucleotides were determined spectrophotometrically using an extinction coefficient of $\epsilon = 8.1 \times 10^3$ M^{-1} (nucleotide) cm^{-1} at 260 nm (Kowalczykowski *et al.*, 1981). Oligonucleotides (10 pmol in a 20-μL reaction volume) were labeled with [γ-^{32}P]ATP (4500 Ci/mmol) using T4 polynucleotide kinase for 1 h at 37 °C (Ausubel *et al.*, 1989). ^{32}P-labeled oligonucleotides were separated from free [γ-^{32}P]ATP using a DuPont Nensorb 20 column according to the manufacturer's instructions.

Buffers. Buffer A is 25 mM Tris-HCl, pH 7.5, 1 mM EDTA, 10% glycerol, 1 mM DTT, and 0.1 mM PMSF. Buffer HI is 30 mM HEPES (diluted from 1 M stock at pH 7.8), 1 mM DTT, 0.25 mM EDTA, 0.5% inositol, and 0.01% NP-40. Buffers contained additional salts as indicated in text. FB buffer is 30 mM HEPES (diluted from 1 M stock at pH 7.8), 100 mM NaCl, 5 mM $MgCl_2$, 0.5% inositol, and 1 mM DTT.

Purification of RPA. RPA was purified using a modification of published procedures (Wold *et al.*, 1989; Brill & Stillman, 1989). Unless noted, all manipulations were carried out at 4 °C. Cytoplasmic extracts (Wold *et al.*, 1989) from 75 L (4.4 g of protein) of HeLa cells were passed over Affi-Gel Blue and single-stranded DNA-cellulose columns as described previously (Brill & Stillman, 1989) except that RPA was eluted using buffers containing NaSCN instead of ethylene glycol. RPA eluted in buffer A with 1.5 M NaSCN from both Affi-Gel Blue and single-stranded DNA-cellulose (Henricksen *et al.*, 1994). 2.6 mg of the 4.4 mg RPA peak from the single-stranded DNA-cellulose column was then loaded onto a hydroxylapatite column (0.5 cm × 1 cm) which had been equilibrated with HI buffer. The column was eluted sequentially with HI buffer with 15 mM sodium phosphate, pH 7.5, 60 mM sodium phosphate, pH 7.5, and 300 mM sodium phosphate, pH 7.5. The peak of RPA (0.96 mg) eluted at 60 mM phosphate and was 90−95% pure. Individual fractions from the HAP peak were subsequently loaded onto a Mono Q HR5/5 column. The column was washed with 4 mL of HI buffer with 100 mM KCl and eluted with a 10-mL gradient from 100−400 mM KCl. RPA eluted at approximately 300 mM and had been purified to >98% purity as indicated by amino acid composition and analysis on an SDS−polyacrylamide gel followed by staining with silver (data not shown). The amino acid composition determined for the purified protein was identical to that predicted by the DNA sequences of the three subunits of RPA (Erdile *et al.*, 1990, 1991; Umbricht *et al.*, 1993) (data not shown). RPA purified by this protocol is completely unphosphorylated (Henricksen *et al.*, 1994). Purified RPA was stored at −80 °C.

Protein Methods. Throughout our studies, protein was quantitated by Bradford assay (Bio-Rad) using bovine serum albumin as a standard (Bradford, 1976). In order to precisely quantitate the amount of RPA, we determined the protein concentration present in four independent preparations of purified RPA by both amino acid analysis and the Bradford assay. We found that the protein concentration obtained by the Bradford assay was 95 ± 16% of the value obtained by amino acid analysis. In all the experiments the protein concentration used was based either upon values obtained by amino acid analysis or upon values obtained by Bradford assay that were corrected by 1/0.95.

DNA Binding Reactions. Binding reactions were carried out as described previously (Kim *et al.*, 1992). Reactions were assembled at 0 °C and then incubated for 30 min at 25 °C. All binding reactions contained indicated amounts of RPA and radioactively labeled oligonucleotides in 15 μL of FB buffer. Individual reactions were analyzed by hydrodynamic methods or separated and quantitated on an agarose gel as described below.

Gel Permeation Chromatography. The sample to be chromatographed was brought to a final volume of either 50 or 200 μL with HI buffer with 200 mM KCl and loaded onto a 24-mL Superose 6 HR10/30 column (Pharmacia) equilibrated in HI buffer with 200 mM KCl. The column was eluted at a flow rate of 0.4 mL/min, and fractions were analyzed by liquid scintillation counting or by SDS−polyacrylamide gel electrophoresis followed by staining with silver.

Glycerol Gradient Sedimentation. The sample to be sedimented was brought to a final volume of either 50 or 200 μL with HI buffer with 200 mM KCl and loaded onto a 5-mL 15−35% glycerol gradient in HI buffer with 200 mM KCl. The gradient was centrifuged at 48 000 rpm in a Beckman SW 55 Ti rotor for 20 h at 4 °C. Parallel gradients containing standard proteins were sedimented in each experiment. The gradients were fractionated from the bottom of the tube using a gradient fractionator (Hoefer Scientific Instruments). Each fraction was analyzed by liquid scintillation counting or by SDS−polyacrylamide gel electrophoresis followed by staining with silver.

Ultraviolet Cross-Linking RPA to Oligonucleotides. RPA (10−500 ng) was incubated with the oligonucleotide indicated (0.02−5 pmol) at 25 °C for 15 min in a total volume of 20 μL of HI buffer with 15 mM KCl. The reaction mixture was transferred to the surface of a piece of Parafilm and irradiated in a Stratalinker model 2400 at 254 nm with 1.25×10^6 μJ/cm^2. The irradiated reaction mixture was transferred to a 1.5-mL microcentrifuge tube and kept at 4 °C until use.

Gel Retardation Assays. Gel mobility shift assays were carried out as described previously (Kim *et al.*, 1992). Individual DNA-binding reactions were brought to a final concentration of 4% (v/v) glycerol and 0.004% (w/v) bromophenol blue and electrophoresed on 1% agarose in 0.1× TAE (1× TAE is 40 mM Tris-acetate, pH 7.8, 1 mM EDTA) for 1−2 h at 10 V/cm at room temperature. In all assays, the gels were dried on Whatman DE81 paper and radioactive bands localized by autoradiography. Each band was excised and the radioactivity measured by liquid scintillation counting.

Fluorescence Titrations. The fluorescence studies were performed on an SLM 4800C spectrofluorometer. All titrations were performed in 2 mL under the same conditions as other binding reactions (FB buffer at 25 °C). The oligonucleotide and poly(dT) titrations were carried out with RPA concentrations of 25−70 nM by adding varying amounts of DNA to a constant concentration of RPA. Protein fluorescence was measured using 282-nm excitation and 348-nm emission. Excitation band path was 2 nm and emission band path was 4 nm. Slit width was 1 nm. In the fluorescence titrations each reading was collected for 5 s after a 1-min period of equilibration. The decrease of fluorescence that occurred without adding DNA, called photobleaching, was determined in independent experiments. All titrations were corrected for dilution and photobleaching as has been described previously (Lohman & Overman, 1985). Normally, in a 15-point titration, up to 10% of initial fluorescence was lost due to photobleaching. Inner filter effects were negligible due to the low concentration of DNA used throughout the entire fluorescence titration.

Calculation of Binding Parameters. Nonlinear least-squares fitting was carried out either using Kaleidagraph (Abelbeck Software) on a Macintosh IIci computer or Nonlin (Johnson & Frasier, 1985) on a Silicon Graphics workstation. All nonlinear analyses were multiply determined using a variety of initial values. Fitting was carried out to the equations listed below with scaling factors added to allow fitting to the experimentally determined end points of each titration.

Bimolecular binding reactions were fit to the Langmuir binding equation. The independent variable in these experiments was either total active RPA or total oligonucleotide; therefore, the Langmuir equation was converted to a function of total active RPA and total DNA using mass balance and equilibrium binding equations (eq 1).

$$\text{fractional saturation} = \frac{(kD_t) + (kR_t + 1) - [((kD_t) + (kR_t))^2 - (4k^2R_tD_t)]^{0.5}}{2k} \quad (1)$$

Where k = association constant, R_t = total active RPA (molar), and D_t = total DNA (molar). When eq 1 was used to fit to binding isotherms in which free DNA had been monitored, data were fit to [(total DNA − calculated fractional saturation)/total DNA].

Cooperativity of binding was determined using two models. (1) A classical two site binding equation (eq 2) that assumes two independent binding sites with possible cooperative interactions between the two sites (Ackers *et al.*, 1983). (2) The nonspecific binding site model developed by Draper and von Hippel (1978). This model (eq 3) considers an oligonucleotide as a series of overlapping binding sites and accounts for both cooperativity and occlusion of possible binding sites

$$\text{fractional saturation} = \frac{(k_1X + 2k_2X^2)}{2(1 + k_1X + k_2X^2)} \quad (2)$$

where X is the free ligand concentration and k_1 and k_2 are macroscopic binding constants that are a combination of the microscopic binding constants. $k_1 = K_1 + K_2$ and $k_2 = K_1K_2\omega$. K_1 = microscopic binding constant for site 1, K_2 = microscopic binding constant for site 2, and ω = cooperativity constant. For RPA binding to oligo(dT) we assumed that $K_1 = K_2$

$$\text{fractional saturation} = \frac{(S_1k_{int}X + 2S_2\omega k_{int}{}^2X^2)}{(1 + S_1k_{int}X + S_2\omega k_{int}{}^2X^2)} \quad (3)$$

where X is the free ligand concentration, k_{int} is the intrinsic binding constant, ω is the cooperativity constant, and S_1 and S_2 are statistical parameters that indicate the number of possible binding sites for the first and second ligands, respectively. The statistical parameter for binding of the first ligand is defined as $S_1 = (l - m + 1)$ where l = the length of the oligonucleotide and m = the binding site size. The statistical parameter for binding of the second ligand, S_2, is equal to the number of potential sites available to the second ligand after the first ligand is bound (Draper & Von Hippel, 1978). We assumed that RPA bound with a single polarity for our analysis.

The Newton−Raphson method was used to determine the concentration of free protein from total protein and DNA concentrations. These calculated free protein concentrations were then fit using eq 2 or 3.

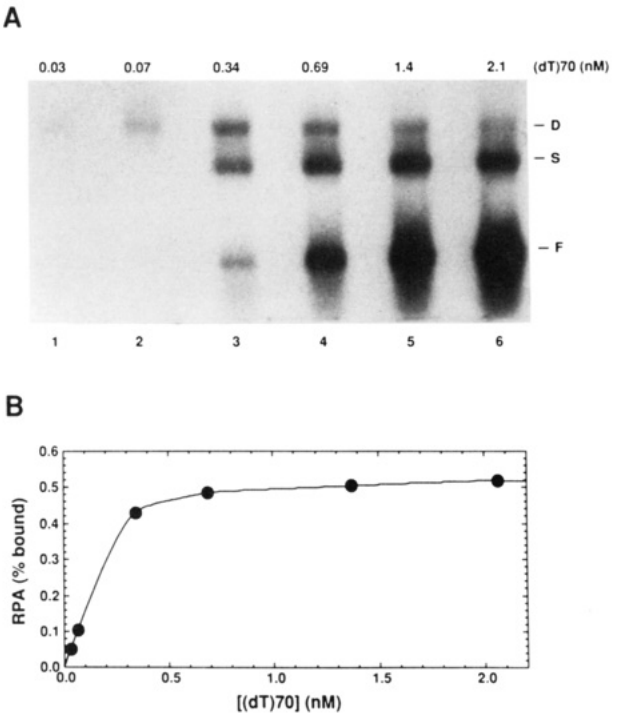

FIGURE 1: Determination of fraction of RPA capable of binding to DNA. Data from a single representative experiment are shown. (A) 66 pM RPA was incubated with indicated concentrations of oligo(dT)70 for 30 min at 25 °C. [Concentrations of oligo(dT)70 (moles fragment) have been rounded off to two digits.] The reactions were separated on a 1% agarose gel as described under Experimental Procedures. Positions of unbound (F), singly-liganded (S), and doubly-liganded (D) (dT)70 are indicated. (B) Quantitation of RPA•oligo(dT)70 titration. Regions of the gel corresponding to free DNA and RPA•DNA complexes were quantitated as described under Experimental Protocols. The number of molecules of RPA bound was assumed to be one per ssDNA molecule for the singly-liganded complex and two for the doubly-liganded complex. Note that in the presence of excess DNA virtually all of the complexes were singly-liganded. Background was determined by counting a similar area below the shifted bands in each lane.

RESULTS AND DISCUSSION

Activity of RPA. RPA was purified from HeLa cell extracts to apparent homogeneity. We next determined the percentage of the purified RPA that was able to bind ssDNA. A constant amount of RPA was incubated with increasing amounts of radiolabeled oligo(dT)70 and the RPA•DNA complexes were quantified by analysis on an agarose gel (Figure 1A). At very low DNA concentrations, the RPA formed a low mobility, doubly-liganded complex with oligo(dT)70 (Figure 1A, lanes 1 and 2). As the concentration of DNA increased, both singly-liganded complex and free DNA were observed (Figure 1A, lanes 3−6). The fraction of RPA bound to DNA is shown in Figure 1B. At saturation, 52% of the RPA heterotrimer present was bound to oligo(dT)70 (Figure 1B). This value remained constant through multiple titrations, and similar values were obtained with oligo(dT)50 and oligo(dT)30 (data not shown). We show below that RPA binds to DNA as a heterotrimer; therefore, we conclude that 52% of the purified RPA protein was capable of binding DNA. This level of activity of RPA was confirmed in stoichiometric titrations (see below). Characterization of multiple independent preparations of RPA indicated that this level of activity was representative. We found that the percentage of active protein varied between 35 and 55% in three different preparations of RPA. We will refer to this fraction of RPA as "active" RPA. In the binding studies presented in this paper, all calculations were made using the concentration of active RPA.

It was possible that the reduced activity of RPA was caused by endogenous ssDNA that had remained associated with the RPA during purification. To test this possibility, samples of RPA were boiled and mixed with polynucleotide kinase and [γ-^{32}P]ATP. Under these conditions, endogenous nucleic acids will become radioactively labeled. No labeling was detected either with or without pretreatment with calf-intestinal phosphatase (data not shown). Control experiments indicated that the level of detection in this assay was 0.04 mol of 5′ termini per mol of RPA (data not shown). We conclude that the reduced activity of the purified protein was not due to the presence of contaminating nucleic acids but rather that some of the RPA had lost activity during purification.

Hydrodynamic analysis indicated that the highly purified RPA used in these studies existed as a single species in solution (see below). This suggests that the inactive RPA was in a near native conformation. The purification procedure utilized two affinity columns (Affi-Gel Blue and ssDNA cellulose). RPA binds with very high affinity to both matrices and requires chaotropic conditions for elution. Thus, it is most likely that some RPA was inactivated by these harsh elution conditions. All published methods of purifying RPA utilize at least one affinity column (Wobbe *et al.*, 1987; Fairman & Stillman, 1988; Wold & Kelly, 1988; Mitsis *et al.*, 1993; Alani *et al.*, 1992). However, the proportion of RPA that retains activity after purification has not been examined previously, so it is not known whether the specific activity of RPA varies significantly between different purification procedures. Specific activity has a major impact on the determination of binding parameters, particularly binding site size. Thus, differences in specific activity could be partially responsible for the different binding properties of RPA observed in different laboratories (Alani *et al.*, 1992; Mitsis *et al.*, 1993; see also *Cooperativity of RPA*, below).

RPA Binds to DNA as a Heterotrimer. RPA exists as a heterotrimer in solution (Wold & Kelly, 1988; Fairman & Stillman, 1988; Kenny *et al.*, 1990). In order to precisely define the structure of RPA•DNA complexes, we carried out hydrodynamic analysis of native RPA and RPA•oligonucleotide complexes. Our preparations of RPA behaved as a single homogeneous species with a Stokes radius of 52.7 Å and a sedimentation coefficient of 5.3 S (Table 1). These values are consistent with previous studies of human RPA (Kenny *et al.*, 1990). Using the procedure of Siegal and Monty (1966), we calculated that RPA has a molecular mass of 117 kDa and an f/f_0 of 1.6 (Table 1). Our calculated mass was slightly larger than predicted by the amino acid sequence but was consistent with the native form of RPA being a 1:1:1 complex.

RPA forms a single complex when it interacts with oligo(dT)30 (Kim *et al.*, 1992). This complex was characterized on a Superose 6 column (Figure 2A). After being incubated with equal amounts of RPA, radiolabeled oligo(dT)30 eluted with a Stokes radius of 55 Å (Figure 2A). This was significantly larger than the radius of free oligo(dT)30 and slightly larger than that of free RPA. Identical results were obtained whether or not the RPA•oligo(dT)30 complexes had been UV-cross-linked prior to separation (data not shown).

Table 1: Hydrodynamic Properties of RPA•Oligonucleotide Complexes[a]

	RPA	RPA•dT30	RPA_1•dT70[b]	RPA_x•dT70[c]
Stokes radius (Å)	52.7 ± 0.5	55 ± 0.5	60.5 ± 0.5	86.5 ± 2
sedimentation coefficient (S)	5.3 ± 0.1	5.75 ± 0.1	5.6 ± 0.1	10.6 ± 0.1
calculated mass (kDa)	117	~133	~142	~385
predicted mass (kDa)	111	126[d]	138[d]	255,[e] 373[f]
f/f_0	1.60	1.63	1.75	1.80
mass (kDa) of oligonucleotide		9	21	21

[a] All values are based upon 2−4 independent experiments. Mass calculated by method of Siegal and Monty (1966). [b] Values are combined from data from (i) binding reactions with equal molar RPA and oligonucleotide and from (ii) the smaller complex observed in experiments containing excess RPA. [c] Values are from the larger complex observed in experiments containing excess RPA. [d] Molecular mass calculated from the sum of mass determined for free RPA and calculated for oligonucleotide. [e] Calculation assumes complex contains two heterotrimers of RPA. [f] Calculation assumes complex contains three heterotrimers of RPA.

The small peaks of radioactive material observed in fractions 36 and 42 were due to radiation-induced fragmentation and residual unincorporated ATP present in this preparation of labeled oligo(dT)30 [see Figure 2A, oligo(dT)30 alone]. RPA•oligo(dT)30 complexes were also analyzed by sedimentation on glycerol gradients (data not shown). To prevent dissociation during separation, RPA•oligo(dT)30 complexes were either cross-linked prior to sedimentation or were sedimented on glycerol gradients containing saturating concentrations of oligo(dT)30 throughout the gradient. Both procedures gave identical results. The RPA•oligo(dT)30 complex had a sedimentation coefficient of 5.75 S and a molecular mass of 133 kDa (Table 1). This is close to the theoretical mass of a complex containing one molecule each of RPA and oligo(dT)30. We conclude that a single RPA heterotrimer binds to oligo(dT)30. In addition, the asymmetry of the RPA•oligo(dT)30 complex was nearly identical to native RPA, suggesting that RPA does not undergo a dramatic conformational change upon binding DNA.

We also characterized the RPA complexes formed upon binding oligo(dT)70. RPA has been shown to form multiple complexes with oligo(dT)70 (Kim *et al.*, 1992; see also Figure 1); therefore, complexes formed at different ratios of RPA to oligo(dT)70 were examined. When equimolar amounts of RPA and oligo(dT)70 were mixed under binding conditions and characterized by gel permeation chromatography, a single major peak with a Stokes' radius of 60.5 Å was observed (Figure 2B). This complex was larger than either RPA or oligo(dT)70 alone. Some radioactivity was also eluted at the position of free oligo(dT)70 indicating that not all of the oligo(dT)70 was complexed with RPA. When oligo(dT)70 was incubated with a 10-fold molar excess of RPA, two peaks with Stokes' radii of 87 Å and 60.5 Å were observed (Figure 2B, fraction 24 and 28, respectively). The 60.5-Å peak eluted at a position identical to the complex formed in the 1:1 binding reactions and corresponded to a singly-liganded complex (see below). The Stokes' radius of the larger, 87-Å peak suggested that it was composed of oligo(dT)70 with multiple molecules of RPA bound. The 87-Å peak was asymmetric, suggesting that more than one multiply-liganded oligo(dT)70 complex may have formed

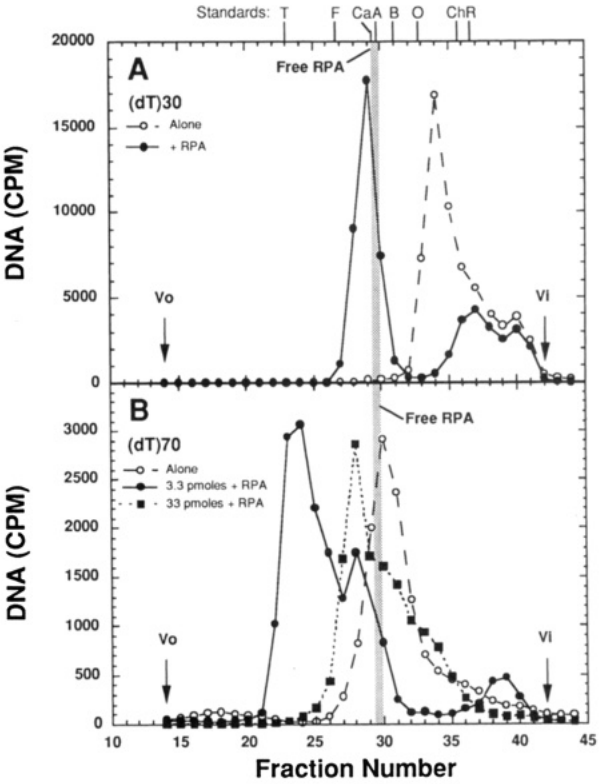

FIGURE 2: Analysis of RPA•DNA complexes by gel permeation chromatography. 68 pmol of RPA was incubated with radiolabeled oligo(dT)30 (A) or oligo(dT)70 (B) and then fractionated on a Superose 6 column. RPA alone had a Stokes radius of 52.7 Å (position indicated by stippled bar). The elution profile of each oligonucleotide alone is shown (open circles, dashed line). The RPA•oligo(dT)30 mixture was UV-cross-linked prior to separation. The single complex formed when RPA was incubated with oligo(dT)30 had a Stokes' radius of 55 Å (closed circles, solid line). When RPA was incubated with an equal amount (33 pmol) of oligo(dT)70, a single complex formed (Stokes' radius of 60.5 Å; closed squares, dotted line). Incubation of oligo(dT)70 with a 10-fold molar excess of RPA resulted in two complexes (Stokes' radii of 87 and 60.5 Å; closed circles, solid line). For each profile, constant volume of each fraction was quantitated by liquid scintillation counting. Standards were thyroglobulin (T), ferritin (F), catalase (Ca), aldolase (A), bovine serum albumin (B), ovalbumin (O), chymotrypsinogen A (Ch), and ribonuclease (R).

under these conditions. Identical results were obtained without UV-cross-linking prior to separation (data not shown). The sedimentation coefficients of these RPA•oligo(dT)70 complexes were also determined after sedimentation on glycerol gradients. Binding reactions containing equimolar amounts of RPA and oligo(dT)70 contained a single complex with a sedimentation coefficient of 5.6 S and binding reactions containing a 10-fold molar excess of RPA contained two complexes with sedimentation coefficients of 5.6 and 10.6 S (data not shown and Table 1). The calculated molecular masses for the RPA•oligo(dT)70 complexes observed are shown in Table 1. The mass of the smaller RPA•oligo(dT)70 complex was consistent with it being composed of a single molecule of RPA bound to oligo(dT)-70. The higher order RPA•oligo(dT)70 complex was found to have a mass consistent with a complex of three heterotrimeric molecules of RPA and one molecule of oligo(dT)-70. The complexes formed with oligo(dT)70 were more elongated than either free RPA or the complex formed with oligo(dT)30. This suggests that when multiple molecules of RPA bind to a single molecule, they align along the DNA.

The stoichiometry of the larger RPA·oligo(dT)70 complex was surprising. In previous gel mobility shift experiments only two RPA·oligo(dT)70 complexes have been observed, suggesting that a maximum of two RPA molecules can bind to oligo(dT)70 (Kim *et al.*, 1992; see also Figure 1A). In view of these results, we reexamined the binding of RPA to oligo(dT)70 by gel retardation assay and found that if RPA is at high concentration and at large excess, a third complex can be observed (data not shown). This complex had a lower mobility than the doubly-liganded complex. We conclude that oligo(dT)70 saturates with either two or three molecules of RPA bound depending upon the concentration of RPA and ratio of RPA to DNA. Previously, we have shown that RPA binds to oligo(dT)50 as a 1:1 complex (Kim *et al.*, 1992). Upon reexamination of this binding reaction, we found that, at very high RPA concentrations, a 2:1 complex with oligo(dT)50 could form (data not shown).

Binding Site Size and Interaction Site Size. The geometry of the interactions of nonspecific, single-stranded DNA-binding proteins with DNA is described by two parameters: occluded binding site and interaction site (Draper & von Hippel, 1978). The former is the length of DNA covered when the protein binds, and the latter is the length of DNA that interacts directly with the protein. We used fluorescence spectroscopy to define these parameters for human RPA. This technique monitors changes in the intrinsic fluorescence of a protein that occur upon binding to DNA and permits direct measurement of protein–DNA interactions. A spectrum of the intrinsic fluorescence of hRPA is shown in Figure 3A. The maximum fluorescent signal was observed when RPA was excited at 282 nm. The emission spectrum had a maximum at 348 nm, which suggests that the signal was primarily due to emission from tryptophan residues. In the presence of poly(dT) the emission peak broadened and the maximum shifted to 320 nm (Figure 3A). 58 ± 2% of the initial fluorescence signal was lost upon addition of saturating concentration of single-stranded poly(dT). This reduction in intrinsic RPA fluorescence will be referred to as quenching. When RPA was titrated with increasing concentrations of oligo(dA)50, fluorescence decreased monotonically (Figure 3B). Similar results were obtained with other oligonucleotides (data not shown). When RPA·oligo(dA)50 complexes were incubated in the presence of high concentrations of NaCl, the initial florescence signal was completely recovered (Figure 3C). Experiments with other short oligonucleotides gave similar results with between 100 and 110% of the initial RPA fluorescence being restored by the addition of NaCl (data not shown). Titration of RPA with NaCl in the absence of exogenous DNA resulted in no significant change in intrinsic fluorescence (data not shown). These experiments demonstrate that the changes in RPA fluorescence observed upon the addition of DNA were caused by a reversible binding reaction and not by aggregation or precipitation of RPA.

When RPA was titrated with poly(dT), quenching varied linearly with poly(dT) concentration at several different RPA concentrations (data not shown). This indicated that binding of RPA was stoichiometric under the conditions used in these experiments. Under stoichiometric binding conditions the ratio of protein to DNA at saturation will correspond to the binding site size of the protein. Figure 4 shows binding data from an RPA titration that have been plotted as percent quenching *versus* the ratio of nucleotides of DNA to active

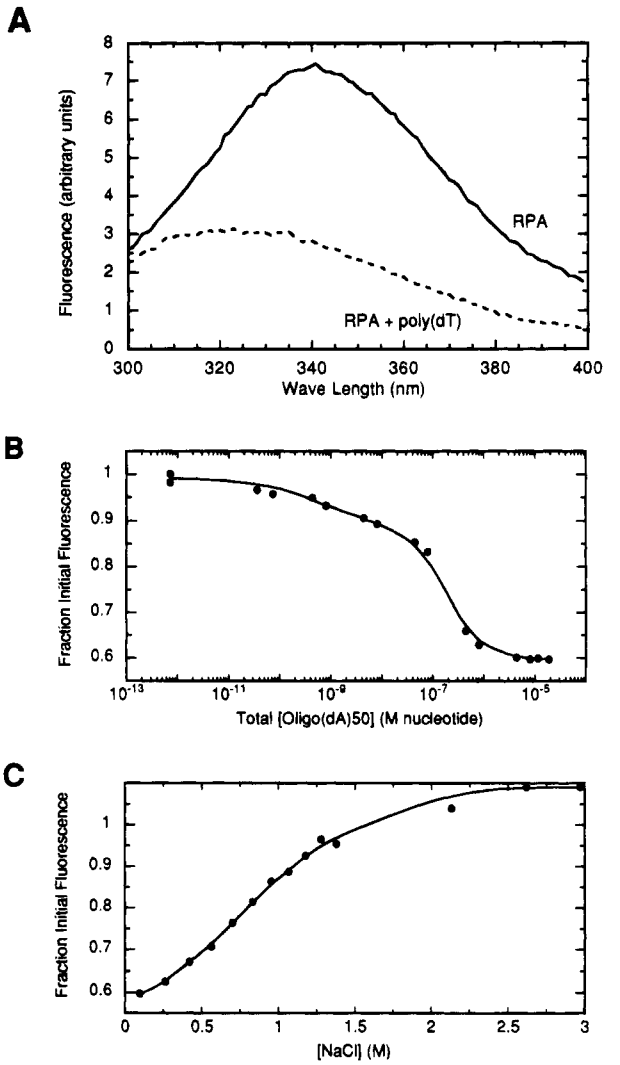

FIGURE 3: Fluorescence properties of RPA. (A) Intrinsic fluorescence spectrum of RPA. Solutions were excited at 282 nm. Fluorescence emission spectrum of RPA solution (4.5 pmol) (solid line) and RPA (4.5 pmol) with poly(dT) (300 pmol of nucleotide) (dashed line). Signal from buffer alone has been subtracted from spectra. (B) Decrease in the intrinsic fluorescence of RPA (32.5 nM) when titrated with oligo(dA)50. (C) Reversal of fluorescence quenching upon the addition of NaCl. Maximally quenched RPA·(dA)50 complexes from panel B were titrated with increasing concentrations of NaCl, and the fluorescence of the solution was monitored. Solid lines in panels B and C are smoothed, interpolated curves.

RPA. As poly(dT) was added to RPA there was a linear increase in quenching up to 30 nucleotides/molecule active RPA (Figure 4). At higher ratios there was no additional change in fluorescence. In multiple experiments with polynucleotides, human RPA heterotrimer had a binding site size of 30 ± 2 nucleotides. Identical results were obtained at several concentrations of RPA (data not shown). These results are consistent with our previous estimate of the binding site size (Kim *et al.*, 1992) and similar to estimates made by other investigators for other mammalian RPAs (Atrazhev *et al.*, 1992; Seroussi & Lavi, 1993).

Binding of RPA to oligonucleotides of different lengths was also examined. We found that maximum quenching obtained with saturating levels of different oligonucleotides varied. Maximum quenching increased linearly with oligonucleotide length from oligo(dT)10 up to oligo(dT)30 and then remained constant for all oligonucleotides longer than

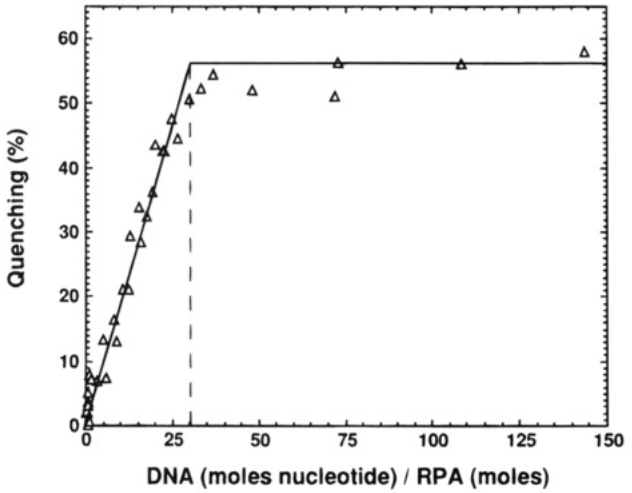

FIGURE 4: Determination of binding site size of RPA by fluorescence quenching. Poly(dT) was added to RPA solution (44.7 nM). The RPA fluorescence was monitored (excitation = 282 nm; emission = 348 nm). Percent quenching (Q) is the absolute fluorescence change normalized by the initial RPA fluorescence in the absence of poly(dT); $(F_o - F_i)/F_o$ where F_o is initial RPA fluorescence and F_i is RPA fluorescence after addition of poly(dT). Calculations were based upon active RPA present.

Table 2: Length Dependence of RPA Binding

oligonucleotide	maximum ouenching[a]	stoichiometry of RPA binding[b]	$K_a \times 10^9$ (M^{-1})
dT10	22%	nd[c]	0.07 ± 0.009[d]
dT12	25%	nd	0.16 ± 0.015[e]
dT15	32%	nd	0.95 ± 0.12[e]
dT20	40%	1	3.7 ± 0.7[e]
dT30	55%	1	4.6 ± 1.0[e]
dT50	nd	nd	15 ± 1.0[e]
dT60	nd	nd	23 ± 2.7[e]
dT70	55%	3	17 ± 1.8[e]
poly(dT)	58%	1/30 nt	nd

[a] Maximum quenching determined from DNA titration as shown in Figure 3. [b] Stoichiometry determined from inflection point of stoichiometric binding reactions monitored by fluorescence titrations as shown in Figure 4. Stoichiometry shown as ratio of moles of active RPA verses moles of DNA fragment. For poly(dT) ratio is in terms of moles of nucleotides. [c] nd, not determined. [d] Binding constant determined from fit of fluorescence titration of RPA with oligo(dT)10 (see text). [e] Binding constants determined from gel mobility shift titrations as described in Figures 6 and 7.

30 nt (Table 2). The highest maximum quenching is likely to occur when all possible interactions have been made and, thus, when the full interaction site is filled by DNA. We conclude that the interaction site size of RPA is between 20 and 30 nucleotides. A schematic diagram of the geometry of RPA binding to ssDNA derived from these studies is shown in Figure 5.

At the protein concentrations necessary to obtain a strong fluorescence signal, we found that RPA also bound stoichiometrically to deoxythymidine oligomers between 15 and 70 nucleotides in length (data not shown). As described above, the inflection point in a stoichiometric titration represents the number of moles of DNA necessary to saturate the protein present. We found that both oligo(dT) 20 and 30 saturated RPA at a molar ratio of one (active heterotrimer/fragment) and that oligo(dT)70 saturated RPA with a molar ratio of three (Table 2). In contrast to longer oligonucleotides, titration of RPA with oligo(dT)10 yielded a hyperbolic binding curve characteristic of an equilibrium binding

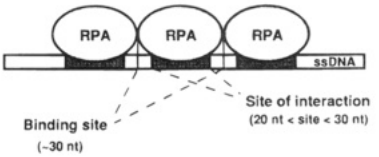

FIGURE 5: Schematic of RPA binding. The figure summarizes the binding site parameters determined for RPA in these studies. Circles representing RPA are shown interacting with ssDNA (horizontal line). Shaded bars represent nonspecific sequences directly interacting with RPA.

reaction (data not shown). By fitting this data to the Langmuir equation, we were able to determine the binding constant of RPA for oligo(dT)10 to be 7×10^7 M^{-1} (Table 2).

In the determination of stoichiometry described in the previous paragraph, only active RPA was considered. The total RPA added was corrected for the experimentally determined activity of 52% (Figure 1). With this correction, the stoichiometry at saturation for each oligonucleotide was an integral molar ratio (Table 2). These stoichiometries were completely consistent with the stoichiometry of RPA·oligonucleotide complexes determined by hydrodynamic studies (Table 1) and in gel mobility shift assays (Kim *et al.*, 1992). If the activity of the RPA differed significantly from the determined value, then nonintegral stoichiometries would have been obtained.

Length Dependence of Binding. A series of gel mobility shift experiments were carried out to quantitate the binding of RPA to oligodeoxythymidine of different lengths. The high sensitivity of gel mobility shift assays means that titrations can be carried out at nanomolar protein concentrations and, thus, under equilibrium binding conditions. We have previously shown RPA·DNA complexes have a mobility different from DNA alone and are stable in this type of gel mobility shift assay (Kim *et al.*, 1992). For each binding reaction in a titration, the amount of radioactive DNA present in each of the observed species was quantitated. By plotting the fraction of total DNA with unaltered mobility (i.e., unbound DNA) verses the concentration of active RPA present, it was possible to generate binding isotherms for each oligonucleotide. Control experiments demonstrated that there was no nuclease present in the RPA fractions used and that no degradation of the input DNA occurred in these experiments (data not shown). In independent experiments, bands with altered mobility were shown to contain RPA by immunoblotting (data not shown).

Figure 6 shows the binding isotherms generated for oligo(dT)12, oligo(dT)30, and oligo(dT)50. In all cases the data fit well to a theoretical curve for a simple bimolecular binding reaction. Table 2 summarizes the binding constants determined from these and other titrations. The apparent binding constant ranged from 1.6×10^8 M^{-1} for oligo(dT)12 to approximately 2×10^{10} M^{-1} for oligonucleotides longer than 50 bases. The increase of binding affinity between 10 and 30 nucleotides is probably caused by the increase in direct interactions between RPA and ssDNA. Oligonucleotides longer than 30 nt (the binding site size of RPA) contain multiple binding sites for RPA and, therefore, the affinity of RPA for longer oligonucleotides would be expected to increase by a statistical factor corresponding to the number of possible binding sites (Draper & Von Hippel, 1978). For example, on an oligonucleotide 50 residues long there are

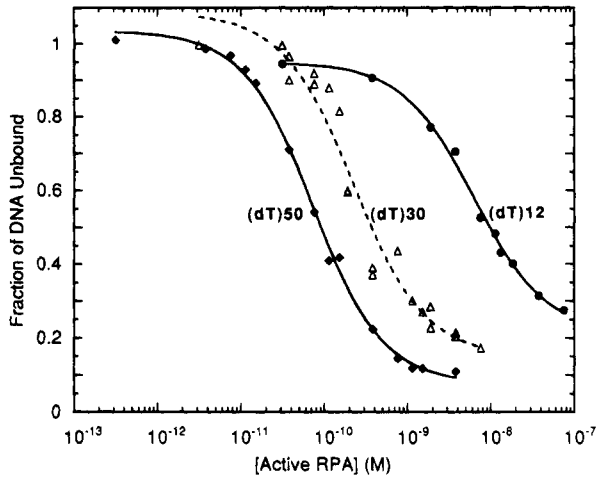

FIGURE 6: Binding isotherms of RPA binding to oligonucleotides of differing lengths. Titrations of different length oligonucleotides with RPA were separated by gel mobility shift assay and then quantified as described under Experimental Procedures. The fraction of free DNA was calculated and displayed as a function of total concentration of active RPA. Data were fit to eq 1. Titration curves for oligo(dT)15 ($K = 9.5 \times 10^8$ M^{-1}), oligo(dT)30 ($K = 4.6 \times 10^9$ M^{-1}), and oligo(dT)50 ($K = 1.5 \times 10^{10}$ M^{-1}) are shown. Lines represent best fitted curves for each data set. Each curve is based upon either data combined from several experiments or one representative titration out of several trials.

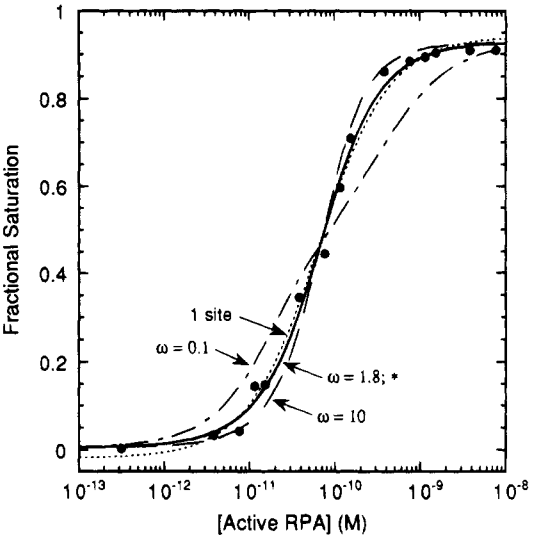

FIGURE 7: Cooperativity of RPA binding to oligo(dT)70. Oligo(dT)70 (1.33×10^{-11} M) was titrated with RPA and each band was quantitated as described under Experimental Procedures. The fractions of DNA bound was calculated by subtracting free DNA from total DNA. The data was fit to various models for RPA binding as described in text. Best fitting theoretical curves shown are for single site binding (eq 1) with $K = 1.76 \times 10^{10}$ M^{-1} (dotted line) and two-site binding (eq 2) with $K = 1.3 \times 10^{10}$ M^{-1}, $\omega = 1.8$ (solid line). To indicate the dependence of the two-site binding upon cooperativity, theoretical curves are shown for $K = 2.5 \times 10^{11}$ M^{-1}, $\omega = 0.1$ (alternating long and short dashes) and for $K = 2.5 \times 10^9$ M^{-1}, $\omega = 10$ (dashed line). All two site curves have constant total free energy of binding. (*) The solid line also represents the best fitted curves obtained using the formation of Draper and von Hippel. Each set of parameters shown in Table 3 gave a curve identical to the solid line.

21 possible binding sites for a protein with a 30 nt binding site. Therefore, on the basis of purely statistical considerations, the affinity of RPA for oligo(dT)50 should be 21-fold higher than that for oligo(dT)30. We observed only a 3-fold increase in binding affinity from oligo(dT)30 to oligo(dT)50. This indicated that the binding of RPA to (dT)50 is not governed by purely statistical factors. Similar nonstatistical behavior was observed with T4 gene 32 protein and interpreted to suggest that T4 gene 32 protein bound preferentially to ends of ssDNA (Kowalczykowski *et al.*, 1981). By analogy, these data suggest that hRPA interacts with short oligonucleotides heterogeneously and may bind preferentially to the ends of DNA.

Our studies have shown that the stoichiometry of RPA binding to oligo(dT)70 at saturation is concentration dependent (see above). The length dependence of RPA binding provides an explanation for these results. RPA has the ability to bind with high affinity to oligonucleotides ≤ 20 residues in length. Thus, RPA would be expected to bind to the exposed ends of DNA present when a single molecule of RPA binds to the end of oligo(dT)50 or to the middle of oligo(dT)70. Since only certain binding events would lead to the higher stoichiometry binding configurations, such binding would not be favored except at high concentrations of RPA.

Cooperativity of RPA Binding. Oligo(dT)70 binds multiple molecules of RPA; therefore, analysis of RPA binding to oligo(dT)70 allowed us to estimate the cooperativity of RPA binding. Only singly- and doubly-liganded complexes were observed in these gel mobility shift assays, so only models with one or two binding events were used to analyze these data. Initially, we fit the data for RPA binding to oligo(dT)70 to the Langmuir equation (eq 1) for a bimolecular binding reaction (see Figure 7, dotted line). Even though RPA binding to oligo(dT)70 consists of multiple binding events, the theoretical curve closely matched the data. This is consistent with each binding event being independent and would imply that there is little cooperativity when RPA binds to short oligonucleotides. We also fit the data to a model that assumed two distinct binding sites with possible cooperativity between sites (eq 2). A close correlation was also found between this model and the binding data (Figure 7, solid line). Optimum values obtained for the two-site binding model were $K = 1.3 \times 10^{10}$ M^{-1} and $\omega = 1.8$, where ω is a unitless cooperativity constant. Increasing or decreasing the cooperativity of binding resulted in curves that deviated significantly from the actual data (Figure 7). This two-site model provides a minimum estimate of the cooperativity of binding. RPA actually binds to ssDNA nonspecifically; therefore, binding of the first molecule of RPA will occlude some potential binding sites for the second molecule of RPA. This occlusion of binding sites results in an apparent negative cooperativity for the binding of a second molecule. This negative cooperativity is not directly considered in the two-site model and leads to a decrease in the cooperativity parameter (ω) when this model is used.

In order to account for overlapping binding sites, we also estimated the cooperativity of RPA binding using a formulation developed by Draper and von Hippel (1978) to describe the interaction of nonspecific binding proteins with short oligonucleotides. This formulation (eq 3) is identical to the two-site model (eq 2) except that it includes two statistical parameters, S_1 and S_2, that depend upon the number of potential binding sites available for the first and second proteins bound, respectively. The statistical parameter for the initial binding event (S_1) is defined by the 30 nt binding site of RPA and the length of the oligonucleotide. The second statistical parameter is more difficult to define

Table 3: Cooperativity Parameters for Binding of RPA to Oligo(dT)70[a]

	model			
	two-site	DvH	DvH	DvH
Minimum Length Bound[b]	30[c]	30[b]	25[b]	20[b]
S_1		41	41	41
S_2		160	272	462
K_{int} ($\times 10^8$ M^{-1})	130 ± 20	2.4 ± 0.6	2.4 ± 0.6	2.4 ± 0.6
ω	1.8 ± 0.7	23.9 ± 16	14.1 ± 9.3	8.3 ± 5.5

[a] Cooperativity parameters were calculated by fitting data for RPA binding to oligo(dT)70 (Figure 7) to either a two-site model (eq 2; two-site) or to the model developed by Draper and von Hippel (1978) (eq 3; DvH). [b] Minimum length bound was operationally defined as the minimum length of ssDNA that RPA would still allow RPA binding at high affinity. This value was used to determine the number of possible sites available for a second binding event (S_2). [c] For the two-site model, both binding sites were defined to be 30 nt.

precisely. When a molecule of RPA binds to oligo(dT)70, the length of the ssDNA segment available to a second molecule will depend upon the specific 30 nt segment bound (e.g., initial binding to the middle of oligo(dT)70 will leave 20 nt segments on either side). Thus, the number of potential binding sites for a second molecule of RPA (which determines S_2) will depend upon the minimum length to which RPA can bind. Our studies demonstrated that RPA can bind to oligonucleotides less than 30 nt long with high but differing affinities (Table 2); therefore, we fit the data using a variety of S_2 parameters based upon different minimum lengths of DNA capable of being bound (Table 3). Minimum binding lengths between 20 and 30 nt all resulted in low values for the cooperativity parameter of RPA (Table 3). For example, using the intermediate minimum binding length of 25 nt, ω was calculated to be ~15 (Table 3). With all sets of parameters used, the best fit curve was identical and correlated well with the data (solid line, Figure 7). Each set of statistical parameters used gave the same intrinsic binding constant for RPA, $K_{int} = 2.4 \times 10^8$ M^{-1}. This value is significantly lower than the intrinsic binding constants obtained with oligo(dT)20 and oligo(dT)30 (Table 2). This difference probably reflects that the Draper and von Hippel model does not completely describe the geometry of RPA binding to short oligonucleotides.

Both of the models used to estimate the cooperativity of RPA binding assume that the binding site size is constant and that all binding sites are equivalent. Both of these assumptions are probably not true for RPA binding. We found that the affinity of RPA for different length oligonucleotides varied significantly. In addition, the difference between the association constant for oligo(dT)30 and oligo(dT)50 is less than would be expected if binding was completely random. This suggests that all binding sites are not equivalent and that RPA may have a preference for binding to the ends of DNA. [It should be noted that if RPA does have a significant preference for binding to ends, then the two-site model used above would accurately describe the binding of RPA to oligo(dT)70.] In spite of the limitations of the models used, we believe that our analyses provide a good initial estimate of the cooperativity of human RPA. All methods of analysis yielded fitted curves that correlated highly with the data, and all indicated that RPA binds with low cooperativity. This would not be the case if RPA binding was highly cooperative. In addition, these results are consistent with previous studies from our laboratory which suggested that RPA binds to ssDNA, including longer oligonucleotides, with low cooperativity (Kim *et al.*, 1992). We conclude that human RPA binds with low cooperativity and has a cooperativity parameter (ω) that is on the order of 15. This level of cooperativity is significantly lower than that of T4 gene 32 protein (ω = ~2000) (Kowalczykowski *et al.*, 1981) and *E. coli* SSB (ω = ~400) (Bujalowski & Lohman, 1987) but similar to the cooperativity of adenovirus DNA-binding protein (ω = 20−30) (Kuil *et al.*, 1989) (see also below).

The binding parameters of the *S. cerevisiae* and *D. melanogaster* homologues of RPA (scRPA and dRPA, respectively) have also been characterized. dRPA has been shown to have a binding site of approximately 22 nucleotides and to bind to ssDNA with low cooperativity (Mitsis *et al.*, 1993). In contrast, scRPA was found to have a binding site of 90−100 nucleotides and to bind with very high cooperativity (Alani *et al.*, 1992). The studies presented here indicate that the binding properties of human RPA are similar to those of dRPA. Because each homologue has been characterized using slightly different conditions and methods, additional studies will be necessary in order to determine the biochemical basis for these differences. scRPA is not able to support SV40 DNA replication. It has been suggested that this species specificity arises as a result of differences in the ability of RPA homologues to form specific protein−protein interactions (Melendy & Stillman, 1993). The variations in the DNA binding properties described above may also contribute to differences in the ability of RPA homologues to support SV40 DNA replication.

During these studies, we found evidence that RPA could aggregate under some conditions. When binding reactions containing 50 nM RPA that had been incubated at 24 °C for 5−30 min were centrifuged at 10 000 *g* for 5 min, approximately half of the RPA present pelleted (data not shown). DNA was also found in the pellet fraction, so we conclude that the aggregated RPA was capable of binding DNA. Aggregation has been observed previously with both dRPA and scRPA (Mitsis *et al.*, 1993; Alani *et al.*, 1992). In the case of dRPA aggregation occurred only at high salt concentrations [>1.7 M NaCl (Mitsis *et al.*, 1993)]. In contrast, we found that aggregation of hRPA was independent of salt concentration (up to 2 M NaCl) but was dependent upon protein concentration (data not shown). In our standard gel mobility shift assays (<10 nM RPA) no aggregation was observed, but when very high concentrations of RPA were used in a gel mobility shift assay (>100 nM), protein complexes were observed that did not enter the gel (data not shown). This suggests that RPA may aggregate only at high concentrations. We have not characterized the structure of these aggregates. They may be either specific multimers or nonspecific aggregates. Electron microscopic studies have shown that scRPA can form nucleosome-like structures either in the presence or absence of DNA (Alani *et al.*, 1992). The conditions used for fixing scRPA prior to examination were quite different from those in our studies; nevertheless, it is possible that the nucleosome-like structures are related to the aggregates we observed.

Human RPA is essential for DNA replication. These studies represent the first detailed analysis of the interactions between hRPA and DNA. These interactions are essential to RPA function, and their characterization should lead to a

better understanding of the molecular mechanisms of DNA replication and the role of RPA in the cell.

ACKNOWLEDGMENT

We thank L. A. Henricksen, X. Gomes, and Z. Sibenaller for scientific discussions and critical reading of the manuscript. We thank Michael Brenowitz for his help with the initial experiments analyzing RPA binding to oligonucleotides. We also thank Madeline Shea for her assistance and constructive criticism of our data analysis. We thank the University of Iowa DNA Core Facility for oligonucleotide synthesis and the University of Iowa Protein Structure Facility for amino acid analysis.

REFERENCES

Ackers, G. K., Shea, M. A., & Smith, F. R. (1983) *J. Mol. Biol. 170*, 223−242.
Adachi, Y., & Laemmli, U. K. (1992) *J. Cell Biol. 119*, 1−15.
Alani, E., Thresher, R., Griffith, J. D., & Kolodner, R. D. (1992) *J. Mol. Biol. 227*, 54−71.
Atrazhev, A., Zhang, S., & Grosse, F. (1992) *Eur. J. Biochem. 210*, 855−865.
Ausubel, F. M., Brent, R., Kingston, R. E., Moore, D. D., Seidman, J. G., Smith, J. A., & Struhl, K. (1989) *Current Protocols in Molecular Biology*, John Wiley & Sons, New York.
Bradford, M. M. (1976) *Anal. Biochem. 72*, 248−254.
Brill, S. J., & Stillman, B. (1989) *Nature 342*, 92−95.
Brill, S. J., & Stillman, B. (1991) *Genes Dev. 5*, 1589−1600.
Brown, G. W., Hines, J. C., Fisher, P., & Ray, D. S. (1994) *Mol. Biochem. Parasitol. 63*, 135−142.
Bujalowski, W., & Lohman, T. M. (1987) *J. Mol. Biol. 195*, 897−907.
Carty, M. P., Levine, A. S., & Dixon, K. (1992) *Mutat. Res. 274*, 29−43.
Carty, M. P., Hauser, J., Levine, A. S., & Dixon, K. (1993) *Mol. Cell. Biol. 13*, 533−542.
Challberg, M. D., & Kelly, T. J. (1989) *Annu. Rev. Biochem. 58*, 671−717.
Collins, K. L., & Kelly, T. J. (1991) *Mol. Cell. Biol. 11*, 2108−2115.
Coverley, D., Kenny, M. K., Munn, M., Rupp, W. D., Lane, D. P., & Wood, R. D. (1991) *Nature 349*, 538−541.
Coverley, D., Kenny, M. K., Lane, D. P., & Wood, R. D. (1992) *Nucleic Acids Res. 20*, 3873−3880.
Din, S.-U., Brill, S. J., Fairman, M. P., & Stillman, B. (1990) *Genes Dev. 4*, 968−977.
Dornreiter, I., Erdile, L. F., Gilbert, I. U., von Winkler, D., Kelly, T. J., & Fanning, E. (1992) *EMBO J. 11*, 769−776.
Draper, D. E., & Von Hippel, P. H. (1978) *J. Mol. Biol. 122*, 339−359.
Dutta, A., Ruppert, J. M., Aster, J. C., & Winchester, E. (1993) *Nature 365*, 79−82.
Erdile, L. F., Wold, M. S., & Kelly, T. J. (1990) *J. Biol. Chem. 265*, 3177−3182.
Erdile, L. F., Heyer, W.-D., Kolodner, R., & Kelly, T. J. (1991) *J. Biol. Chem. 266*, 12090−12098.
Fairman, M. P., & Stillman, B. (1988) *EMBO J. 7*, 1211−1218.
Fang, F., & Newport, J. W. (1993) *J. Cell Sci. 106*, 983−994.
Georgaki, A., Strack, B., Podust, V., & Hübscher, U. (1992) *FEBS Lett. 308*, 240−244.
He, Z., Brinton, B. T., Greenblatt, J., Hassell, J. A., & Ingles, C. J. (1993) *Cell 73*, 1223−1232.
Henricksen, L. A., Umbricht, C. B., & Wold, M. S. (1994) *J. Biol. Chem. 269*, 11121−11132.
Heyer, W.-D., Rao, M. R. S., Erdile, L. F., Kelly, T. J., & Kolodner, R. D. (1990) *EMBO J. 9*, 2321−2329.
Hurwitz, J., Dean, F. B., Kwong, A. D., & Lee, S.-H. (1990) *J. Biol. Chem. 265*, 18043−18046.
Johnson, M. L., & Frasier, S. G. (1985) *Methods Enzymol. 117*, 301−342.
Karpel, R. L. (1990) in *The Biology of Nonspecific DNA−Protein Interactions* (Revzin, A., Ed.) pp 103−130, CRC Press, Boca Raton, FL.
Kenny, M. K., Schlegel, U., Furneaux, H., & Hurwitz, J. (1990) *J. Biol. Chem. 265*, 7693−7700.
Kim, C., Snyder, R. O., & Wold, M. S. (1992) *Mol. Cell. Biol. 12*, 3050−3059.
Kornberg, A., & Baker, T. A. (1992) *DNA Replication*, W. H. Freeman and Company, New York.
Kowalczykowski, S. C., Lonberg, N., Newport, J. W., & Von Hippel, P. H. (1981) *J. Mol. Biol. 145*, 75−104.
Kuil, M. E., Van Amerongen, H., Van der Vliet, P. C., & Van Grondelle, R. (1989) *Biochemistry 28*, 9795−9800.
Lee, S.-H., Pan, Z.-Q., Kwong, A. D., Burgers, P. M. J., & Hurwitz, J. (1991) *J. Biol. Chem. 266*, 22707−22717.
Li, R., & Botchan, M. R. (1993) *Cell 73*, 1207−1221.
Lohman, T. M., & Overman, L. B. (1985) *J. Biol. Chem. 260*, 3594−3603.
Lohman, T. M., & Bujalowski, W. (1990) in *The Biology of Nonspecific DNA−Protein Interactions* (Revzin, A., Ed.) pp 131−170, CRC Press, Boca Raton, FL.
Melendy, T., & Stillman, B. (1993) *J. Biol. Chem. 268*, 3389−3395.
Mitsis, P. G., Kowalczykowski, S. C., & Lehman, I. R. (1993) *Biochemistry 32*, 5257−5266.
Moore, S. P., Erdile, L., Kelly, T., & Fishel, R. (1991) *Proc. Natl. Acad. Sci. U.S.A. 88*, 9067−9071.
Murakami, Y., Eki, T., & Hurwitz, J. (1992) *Proc. Natl. Acad. Sci. U.S.A. 89*, 952−956.
Nakagawa, M., Tsukada, S., Soma, T., Shimuzu, Y., Miyake, S., Iwamatsu, A., & Sugiyama, H. (1991) *Nucleic Acids Res. 19*, 4292.
Revzin, A., Ed. (1990) *The Biology of Nonspecific DNA−Protein Interactions*, CRC Press, Boca Raton, FL.
Roberts, J. D., Nguyen, D., & Kunkel, T. A. (1993) *Biochemistry 32*, 4083−4089.
Seo, Y.-S., Lee, S.-H., & Hurwitz, J. (1991) *J. Biol. Chem. 266*, 13161−13170.
Seroussi, E., & Lavi, S. (1993) *J. Biol. Chem. 268*, 7147−7154.
Siegal, L. M., & Monty, K. J. (1966) *Biochim. Biophys. Acta 112*, 346−362.
Stigger, E., Dean, F. B., Hurwitz, J., & Lee, S.-H. (1994) *Proc. Natl. Acad. Sci. U.S.A. 91*, 579−583.
Stillman, B. (1989) *Annu. Rev. Cell Biol. 5*, 197−245.
Thömmes, P., Ferrari, E., Jessberger, R., & Hübscher, U. (1992) *J. Biol. Chem. 267*, 6063−6073.
Tsurimoto, T., & Stillman, B. (1989) *EMBO J. 8*, 3883−3889.
Umbricht, C. B., Erdile, L. F., Jabs, E. W., & Kelly, T. J. (1993) *J. Biol. Chem. 268*, 6131−6138.
Williams, K. R., & Chase, J. W. (1990) in *The Biology of Nonspecific DNA−Protein Interactions* (Revzin, A., Ed.) pp 197−227, CRC Press, Boca Raton, FL.
Wobbe, C. R., Weissbach, L., Borowiec, J. A., Dean, F. B., Murakami, Y., Bullock, P. & Hurwitz, J. (1987) *Proc. Natl. Acad. Sci. U.S.A. 84*, 1834−1838.
Wold, M. S., & Kelly, T. (1988) *Proc. Natl. Acad. Sci. U.S.A. 85*, 2523−2527.
Wold, M. S., Weinberg, D. H., Virshup, D. M., Li, J. J., & Kelly, T. J. (1989) *J. Biol. Chem. 264*, 2801−2809.